Carcinogenesis vol.32 no.4 pp.568–575, 2011
doi:10.1093/carcin/bgr021
Advance Access publication February 8, 2011

2′-Hydroxyflavanone inhibits proliferation, tumor vascularization and promotes normal differentiation in *VHL*-mutant renal cell carcinoma

Lokesh Dalasanur Nagaprashantha†, Rit Vatsyayan†, Jyotsana Singhal, Poorna Lelsani, Laszlo Prokai, Sanjay Awasthi and Sharad S.Singhal*

Department of Molecular Biology and Immunology, University of North Texas Health Science Center, Fort Worth, TX 76107, USA

*To whom correspondence should be addressed. Tel: +1 817 735 2236; Fax: +1 817 735 2118;
Email: sharad.singhal@unthsc.edu

Renal cell carcinoma (RCC) is one of the top ten cancers prevalent in USA. Loss-of-function mutations in the von Hippel–Lindau (*VHL*) gene constitute an established risk factor contributing to 75% of total reported cases of RCC. Loss-of-*VHL* leads to a highly vascularized phenotype of renal tumors. Intake of citrus fruits has been proven to reduce the risk of RCC in multicenter international studies. Hence, we studied the effect of 2′-hydroxyflavanone (2HF), an active anticancer compound from oranges, in RCC. Our *in vitro* investigations revealed that 2HF suppresses *VHL*-mutant RCC to a significantly greater extent than *VHL*-wild-type RCC by inhibiting epidermal growth factor receptor signaling, which is increased due to *VHL* mutations in RCC. Our results also revealed for the first time, that 2HF inhibits glutathione S-transferase pi activity. 2HF reduced cyclin B1 and CDK4 levels and induced G_2/M phase arrest in *VHL*-mutant RCC. Importantly, 2HF inhibited the angiogenesis in *VHL*-mutant RCC by decreasing vascular endothelial growth factor expression. Our *in vivo* studies in mice xenografts confirmed our *in vitro* results as evident by decreased levels of proliferation marker, Ki67 and angiogenic marker, CD31, in 2HF-treated mice xenografts of *VHL*-mutant RCC. 2HF also increased the expression of E-cadherin in *VHL*-mutant RCC, which would be of significance in restoring normal epithelial phenotype. Collectively, our *in vitro* and *in vivo* results revealed the potent antiproliferative, antiangiogenic and prodifferentiation properties of 2HF in *VHL*-mutant RCC, sparing normal cells, which could have significant implications not only in the specific management of *VHL*-mutant RCC but also towards other *VHL* syndromes.

Introduction

Renal cell carcinoma (RCC) is a frequently lethal cancer that affects patients who carry inherited or somatic mutations in the von Hippel–Lindau (*VHL*) gene, which contributes to 75% of total RCCs (1–3). RCC arises from epithelial cells of the proximal renal nephron and is characterized by its many different cytological and histological variants (3). Tumor vascularity is of specific significance in RCC because of constitutively active hypoxic signaling in majority of renal tumors as a consequence of *VHL* mutations. According to National Cancer Institute, 1 in 67 men and women harbor the lifetime risk for RCC. Current chemotherapeutic choices for the advanced kidney cancer are limited, with a low chance of temporary remission, small improvement in average survival and substantial toxicity (4). The association of lifestyle habits like tobacco smoking with RCC along with the increased risk for RCC in *VHL*-mutant populations makes the chemoprevention of RCC an important public health necessity (3–5). In this regard, validation of the potential *VHL*-mutant RCC-specific anticancer compounds attains contemporary significance in renal oncology.

Flavonoids are a large group of polyphenolic compounds present in foods and beverages of plant origin, which have antioxidant, anti-inflammatory, antimutagenic and antiproliferative properties (6–8). 2′-Hydroxyflavanone (2HF) is a flavanone belonging to the larger family of flavonoids. The multicenter international RCC studies have established that the intake of citrus fruits is associated with decreased risk of RCC (9). 2HF is known for its antimetastatic effects in lung cancer (10). In the present report, we show that 2HF, an active anticancer compound in oranges and citrus fruits, predominantly inhibits the growth of *VHL*-mutant RCC, a major subtype of RCC. Our investigations addressed the impact of 2HF on oncogenic processes of importance in loss-of-*VHL* induced renal carcinogenesis like regulation of tumor proliferation and specifically angiogenesis in addition to investigating the impact on differentiation of 2HF-treated *VHL*-mutant RCC tumors *in vivo*. Our collective *in vitro* and *in vivo* investigations elucidated the anticancer potential and novel mechanisms of action of 2HF in *VHL*-mutant RCC.

Abbreviations: AKR1C1, aldoketo reductase family 1, member C1; EGFR, epidermal growth factor receptor; GSTπ, glutathione S-transferase pi; 2HF, 2′-hydroxyflavanone; MTT, 3-(4,5-dimethylthiazole-2-yl)-2,5-diphenyl tetrazolium bromide; RCC, renal cell carcinoma; TUNEL, terminal deoxynucleotidyl-transferase deoxyuridine triphosphate nick-end labeling; VEGF, vascular endothelial growth factor; VHL, von Hippel–Lindau.

†These authors contributed equally to this work.

Materials and methods

Reagents

3-(4,5-Dimethylthiazole-2-yl)-2,5-diphenyl tetrazolium bromide (MTT) and 2HF were obtained from Sigma (St Louis, MO). AKRIC, *VHL*, CD31, Ki67, cyclin B1, CDK4, Akt, epidermal growth factor receptor (EGFR), PI3K and E-cadherin antibodies were purchased from Santa Cruz Biotechnology (Columbus, OH) and Cell Signaling Technologies (Danvers, MA). ELISA kit for vascular endothelial growth factor (VEGF) expression was procured from R&D Systems. Source of glutathione S transferase π (GSTπ) antibody was the same as described previously (11). Matrigel was procured from BD Biosciences (San Jose, CA). Terminal deoxynucleotidyl-transferase deoxyuridine triphosphate nick-end labeling (TUNEL) fluorescence and avidin/biotin complex (ABC) detection kits were purchased from Promega (Madison, WI) and Vector (Burlingame, CA), respectively.

Cell lines and cultures

Human RCCs (Caki-2) was purchased from American Type Culture Collection (Manassas, VA), and Caki-1, A-498 and 786-O cells were kindly authenticated and provided by Dr William G.Kaelin, Dana–Farber Cancer Institute, Harvard Medical School, Boston, MA. Human kidney normal (mesangial) cells were a generous gift from Dr Rong Ma, University of North Texas Health Science Center (Fort Worth, TX). All cells were cultured at 37°C in a humidified atmosphere of 5% CO_2 in RPMI-1640 medium supplemented with 10% fetal bovine serum and 1% P/S solution. All cells were tested for *Mycoplasma* once every 3 months.

Proteomic analysis, database searching and comparison of protein expression levels

RCC cells were lysed in buffer containing 20 mM Tris–HCl, 50 mM NaCl and 6 M urea, 10 mM NaPP, 1 mM NaF and 1 mM Na_3VO_4. The lysate (200 μg protein) was subjected to reduction and alkylation of cysteines using 2.5 mM dithiothreitol and 7 mM idoacetamide followed by trypsin digestion and solid phase extraction using a C_{18} cartridge (Supelco, Bellefonte, PA). The digested peptides were analyzed using reverse-phase liquid chromatography-tandem mass spectrometry analysis using a hybrid Linear ion trap (LTQ)–Fourier transform ion cyclotron resonance (FTICR, 7T) mass spectrometer (LTQFT; Thermo, San Jose, CA), which is equipped with nanospray ionization source and operated by XCalibur (version 2.2) data acquisition software as described previously (12). A 120 min gradient provide by nano-LC 2D (Eksigent, Dublin, CA) was carried out to 40% acetonitrile at 250 nl/min. An electrospray ionization spray voltage of 2.0 kV and a capillary temperature of 250°C were maintained during the run. We employed a data-dependent mode of acquisition in which accurate mass/charge (*m/z*) survey scan was done in FTICR cell followed by a parallel MS/MS linear ion trap analysis. FTICR full-scan mass

spectra were acquired at 100 000 mass resolving power (at *m/z* 400) from *m/z* 350 to 1500 using the automatic gain control mode of ion trapping. Collision-induced dissociation in the linear ion trap was performed using a 3.0 Tn isolation width and 35% normalized collision energy with helium as the collision gas. MS/MS spectra were searched against a human protein database by the Mascot software (Matrix Science, Boston, MA) and label-free semiquantitative analysis was guided first by normalized spectral counts from the Scaffold program (Proteome Software, Portland, OR) with previously validated method (12). Extracted ion chromatograms (areas under the corresponding chromatographic peaks) of isoform-specific doubly or triply charged tryptic peptides from the full-scan high-resolution mass spectra were then used as quantitative measures of respective protein expression levels selected for evaluation in this study.

Drug sensitivity (MTT) assay

Cell density measurements were performed using a hemocytometer to count reproductive cells resistant to staining with trypan blue. Approximately 20 000 cells were plated into each well of 96-well flat-bottomed microtiter plates. After 12 h incubation at 37°C, medium containing 2HF (ranging 0–200 μM) were added to the cells. After 72 h incubation, 20 μl of 5 mg/ml MTT were introduced to each well and incubated for 2 h. The plates were centrifuged and medium was decanted. Cells were subsequently dissolved in 100 μl dimethyl sulfoxide with gentle shaking for 2 h at room temperature, followed by measurement of optical density at 570 nm (13–15). Eight replicate wells were used at each point in each of three separate measurements.

Colony formation assay

Cell survival was evaluated using a standard colony-forming assay. In total, 1×10^5 cells/ml were incubated with 2HF (50 μM) for 24 h, and aliquots of 50 or 100 μl were added to 60 mm size petri dishes containing 4 ml culture medium. After 10 days, adherent colonies were fixed, stained with 0.5% methylene blue for 30 min and colonies were counted using the Innotech Alpha Imager HP (16).

Effect of 2HF on apoptosis by TUNEL assay

In total, 1×10^5 cells were grown on the coverslips for ~12 h followed by treatment with 2HF (50 μM) for 24 h. Apoptosis was determined by the labeling of DNA fragments with TUNEL assay using Promega apoptosis detection system according to the protocol described previously (15).

Flow cytometry analysis

The effect of 2HF on cell cycle distribution was determined by fluorescence activated cell sorting analysis. In total, 2×10^5 cells were treated with 2HF (ranging from 25 to 50 μM) for 18 h at 37°C. After treatment, floating and adherent cells were collected, washed with phosphate-buffered saline and fixed with 70% ethanol. On the day of flow analysis, cell suspensions were centrifuged, counted and same numbers of cells were resuspended in 500 μl phosphate-buffered saline in flow cytometry tubes. Cells were then incubated with 2.5 μl of RNase (stock 20 mg/ml) at 37°C for 30 min after which they were treated with 10 μl of propidium iodide (stock 1 mg/ml) solution and then incubated at room temperature for 30 min in the dark. The stained cells were analyzed using the Beckman Coulter Cytomics FC500, Flow Cytometry Analyzer. Results were processed using CXP2.2 analysis software from Beckman Coulter.

In vitro migration assay

Cell migration was determined using a scratch assay (17). In total, 2×10^4 Caki-2 and 786-O cells were seeded in six-well plates to reach 100% confluence within 24 h and then treated with 10 μM mitomycin C for 2 h. Subsequently, a similarly sized scratch was made with a 200 μl pipette tip across the center of each well and immediately imaged at baseline and then at 24 h under an Olympus Provis AX70 microscope. The rate of cell migration was determined by comparing the sizes of scratch area using Image J software.

In vitro angiogenesis assay (tube formation assay)

Tube formation assay was performed as follows: 96-well plates were coated with 100 μl of Matrigel (10 mg/ml) and incubated at 37°C for 30 min to promote gelling. Fourteen thousand cells were resuspended in medium (serum concentration 10%) and added to each well. Tube formation in the presence of 50 μM 2HF was compared. The number and length of tubes formed were counted under an Olympus Provis AX70 microscope for analysis between both the groups.

Assessment of angiogenesis, proliferation and apoptosis

Renal tumors (control as well as 2HF treated) were harvested from mice-bearing tumors for 60 days. Tumor samples fixed in buffered formalin for 12 h were processed conventionally for paraffin-embedded tumor sections (5 μm thick). Hematoxylin and eosin staining was performed on paraffin-embedded tumor sections. Histopathologic analyses with anti-E-cadherin, anti-CD31 and anti-Ki67 IgG were also performed, using Universal ABC detection kit (Vector). The sections were examined under Olympus Provis AX70 microscope connected to a Nikon camera.

In vivo xenograft studies

Hsd: athymic nude nu/nu mice were obtained from Harlan (Indianapolis, IN) and were acclimated for a week before beginning the experiment. All animal experiments were carried out in accordance with a protocol approved by the Institutional Animal Care and Use Committee (IACUC). Twenty-eight 11-weeks-old mice were divided into four groups of seven animals (treated with vehicle only i.e. corn oil and 2HF at the doses of 0.0025, 0.005 and 0.01% wt/wt). All 28 animals were injected with 2×10^6 786-O (*VHL* mutant) cells in 100 μl of phosphate-buffered saline, subcutaneously into one flank of each mouse. At the same time, animals were randomized into control and treatment groups. Treatment was started 10 days after the 786-O cells implantation to see palpable tumor growth. Treatment consisted of 2HF at the doses of 0.0025, 0.005 and 0.01% (wt/wt), equivalent to 25, 50 and 100 mg/kg body wt. respectively, in 200 μl corn oil by oral gavage alternate day. Control groups were treated with corn oil only. In parallel, we also performed Caki-2 (*VHL*-wild-type) RCC xenografts studies. Animals were examined daily for signs of tumor growth. Tumors were measured in two dimensions using calipers and body weights were recorded. Each mouse in every group was monitored on alternate days for signs of distress and areas of swelling or redness. Photographs of animals were taken at day 1, day 10, day 20, day 40 and day 60 after subcutaneous injection are shown for all groups. Photographs of tumors were also taken at day 60.

Statistical analyses

All data were evaluated with a two-tailed unpaired Student's t-test or compared by one-way analysis of variance and are expressed as the mean ± standard deviation. A *P*-value of <0.05 was regarded as statistically significant.

Results

2HF inhibits proliferation and stimulates apoptosis in VHL-mutant RCC

The MTT assay following the treatment of 2HF in RCC cell lines revealed the potent inhibition of survival of *VHL*-mutant RCC in the presence of 2HF [IC_{50} at 72h: *VHL*-mutant RCC (786-O and A498): 28 ± 4 μM, *VHL*-wild-type RCC (Caki-1 and Caki-2): 90 ± 6 μM] (Figure 1A). In accordance with MTT assay, 2HF inhibited the clonogenic survival of *VHL*-mutant RCC (~70% inhibition) in colony formation assay to significantly greater extent when compared with *VHL*-wild-type RCC cells (~20% inhibition) (Figure 1B). Following our initial investigations in four RCC cell lines, we investigated the detailed mechanisms of action of 2HF in Caki-2 (*VHL* wild-type) and 786-O (*VHL* mutant) cells. Our initial cytotoxicity studies revealed that 2HF inhibits the growth of *VHL*-mutant RCC to a greater extent when compared with its inhibitory effect on *VHL*-wild-type RCC. Hence, we focused on investigating the preceding cellular events that determine the eventual cytotoxicity of 2HF in RCC. The cytotoxicity of 2HF treatment was also determined at 24 h by the MTT assay (IC_{50} at 24 h: 786-O = 72 ± 6 μM, caki2 = 148 ± 11 μM). We used 50 μM of 2HF for 24 h treatment for both the cell lines as cell death should be minimal for mechanistic and imaging studies focused on early cellular events that contribute to eventual cytotoxicity at 72 h. The 50 μM of 2HF treatment for 24 h effectively induced apoptosis in *VHL*-mutant RCC to a greater extent, sparing normal mesangial cells, when compared with *VHL*-wild-type RCC as determined by enhanced DNA fragmentation in TUNEL apoptotic assay (Figure 1C). The enhanced cytotoxicity of 2HF in *VHL*-mutant RCC along with the absence of any cytotoxicity towards normal mesangial cells in MTT, clonogenic survival and TUNEL apoptotic assays revealed that 2HF is a potential flavonoid that could have significant therapeutic relevance in specifically targeting *VHL*-mutant RCC.

2HF inhibits activation of EGFR, PI3K and Akt signaling in VHL-mutant RCC

Loss-of-*VHL* leads to upregulation of EGFR signaling in renal cancers (18). Activation of EGFR is involved in the growth and progression of many types of solid tumors, including RCC by upregulating PI3K and Akt signaling (19). Hence, we investigated the effect of 2HF

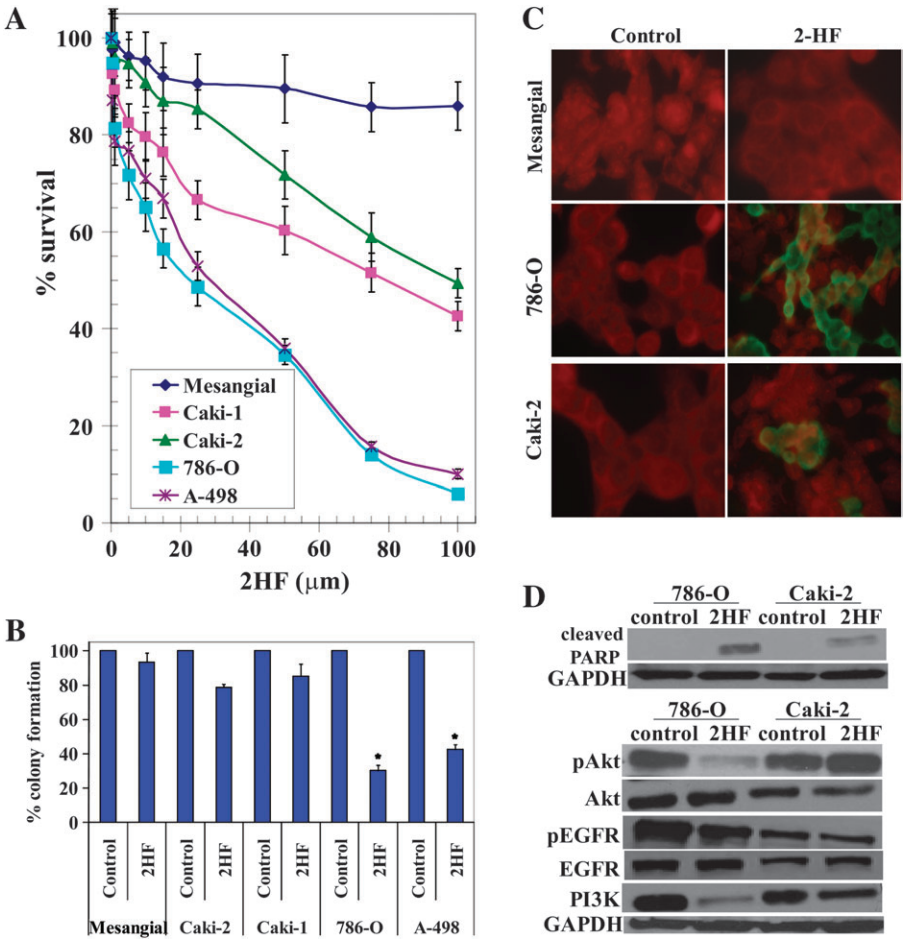

Fig. 1. Enhanced anticancer effects of 2HF in *VHL*-mutant RCC sparing normal cells. Drug sensitivity assays were performed by MTT assay using 2HF at 72 h posttreatment to determine IC_{50}. Values are presented as mean ± standard deviation from two separate determinations with eight replicates each (n = 16) (panel A). Colony-forming assay was performed and the colonies were counted using Innotech Alpha Imager HP as detailed in Materials and Methods. $^{*}P < 0.001$ compared with control (panel B). For TUNEL apoptosis assay, cells were grown on coverslips and treated with 50 μM 2HF for 24 h. TUNEL assay was performed using Promega fluorescence detection kit and examined using Zeiss LSM 510 META laser scanning fluorescence microscope with filters 520 and >620 nm. Photographs taken at identical exposure at ×400 magnification are presented. Apoptotic cells showed green fluorescence (panel C). Effect of 2HF on poly ADP-ribose polymerase cleavage, EGFR, PI3K and Akt activation: *VHL*-wild-type (Caki-2) and *VHL*-mutant (786-O) control and 50 μM 2HF-treated cells were lysed and analyzed by western blot for poly ADP-ribose polymerase cleavage, pEGFR (Y^{1068}), pAkt (S^{473}) and PI3K ($Y^{458}/^{199}$) by using specific antibodies. Membranes were stripped and reprobed for glyceraldehyde 3-phosphate dehydrogenase as a loading control (panel D).

on EGFR signaling in *VHL*-mutant RCC. Western blot analysis revealed that 2HF significantly inhibits pEGFR (Y^{1068}), PI3K ($Y^{458/199}$) and pAkt (S^{473}) in *VHL*-mutant RCC (Figure 1D). The 2HF treatment also increased poly ADP-ribose polymerase-cleavage in *VHL*-mutant RCC (786-O) to a significantly greater extent when compared with *VHL*-wild-type (Caki-2) RCC.

Detection of differential expression of AKR1C1 and GSTπ in RCC

In order to understand the differences in the *VHL*-wild-type and *VHL*-mutant RCC, we performed proteomic analysis of whole cell proteome using a hybrid linear ion trap–Fourier transform ion cyclotron resonance tandem mass spectrometer (LTQFT; Thermo) operated with nano-electrospray ionization and coupled to an Eksigent nano-LC system (12). MS/MS spectra were searched against a human protein database by the Mascot software (Matrix Science) and label-free quantification was guided first by spectral counts from the Scaffold software (Proteome Software, Version 2) with our previously validated method (12). Caki-2 (*VHL* wild-type) and 786-O (*VHL* mutant) cells, revealed differential expression of aldoketo reductase family 1, member C1 (AKR1C1; selectively detected in Caki-2 RCC) and GSTπ (selectively detected in 786-O RCC). The MS/MS spectra of isoforms-specific representative peptides for these proteins are shown in the top with corresponding peptide sequence below (Figure 2A). The relative quantification based on integrated extracted ion chromatograms of doubly and triply charged tryptic peptides detected for AKR1C1 and GSTπ, respectively, are represented in the bar diagrams. This observed differential expression of AKR1C1 and GSTπ was also revalidated by western blot analysis using specific antibodies (Figure 2B).

2HF inhibits GSTπ activity, angiogenesis and migration of VHL-mutant RCC

The enhanced growth inhibitory effect of 2HF, a well characterized AKR1C family inhibitor, in *VHL*-mutant RCC which does not express AKR1C1 was an interesting finding (20). We investigated the effect of 2HF on the enzymatic activity of GSTπ towards GSH and 1-chloro 2,4-dinitro benzene (1, chloro 2, 4-dinitro benzene), a model substrate routinely used for GST activity (11). 2HF inhibited the total GST activity to a significant extent in the *VHL*-mutant RCC (Figure 3A). Human recombinant purified GSTπ was used as a standard in enzyme activity assay (Figure 3A inset). GSTπ is a phase II detoxifying enzyme, which mediates xenobiotic resistance by detoxifying administered chemotherapy drugs for efflux out of cells by transport proteins. GSTπ is an established marker of many aggressive cancers like lung and prostate cancers (21,22). GSTπ-mediated detoxification of toxic end products of

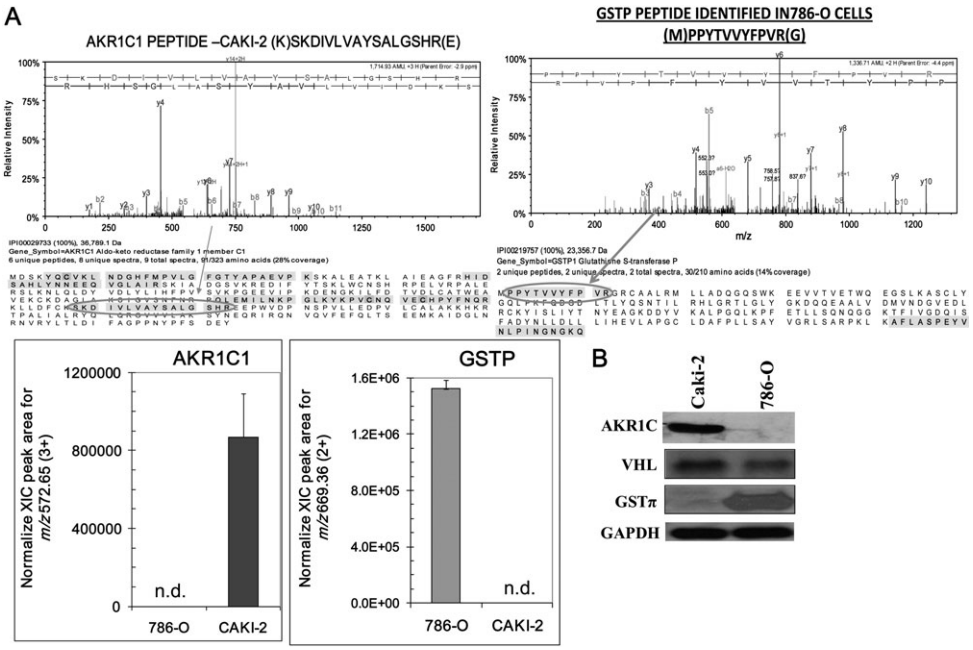

Fig. 2. Differential expression of AKR1C1 and GSTπ in RCC as detected by LC-MS and MS/MS. Caki-2 and 786-O cells were subjected to proteomic analyses as described in Methods section. MS spectra were searched against a human protein database by Mascot software (Matrix Science) and label-free quantification: upper panel shows the MS/MS spectrum of one of the sequenced, isoforms-specific tryptic peptides for the respective proteins with the sequence coverage displayed below. The bar diagrams indicating the quantitative levels of AKR1C1 and GSTπ, respectively, were based on integration of extracted ion chromatograms, n = 4 in each group, for the triply and doubly charged isoform-specific tryptic peptides; n.d. denotes that the peptide was not detected in the samples (panel A). Differential protein expression was confirmed by performing western blot using 50 μg of cell lysates and antibodies against AKR1C, GSTπ and *VHL*. for glyceraldehyde 3-phosphate dehydrogenase was used as internal loading control. The experiment was repeated three times and similar results were obtained (panel B).

lipid peroxidation like 4-Hydroxy-2-nonenal (4-HNE) leads to buffering of tumor-toxic oxidative stress and favors tumor survival and proliferation in hypoxic environment (23). GSTπ also has posttranslational regulatory role in S-glutathionylation of various cell proteins, which is implicated in regulating cell adhesion and proliferation (24). In this regard, the ability of 2HF to inhibit GSTπ and total GST activity in *VHL*-mutant RCC, which has high levels of expression of GSTπ represents an important anticancer effect of 2HF given its cytotoxic potential in *VHL*-mutant RCC. Further detailed studies would reveal the role of GSTπ and oxidative stress pathways in mediating the anticancer effects of 2HF in RCC. As there are no chemopreventive strategies reported for the *VHL*-mutant RCC, which is a highly prevalent malignancy in USA and given the ability of 2HF to effectively inhibit the survival of *VHL*-mutant RCC as revealed by our initial studies, we specifically focused on studying the impact of 2HF in regulating the proliferative potential, angiogenic response and differentiation of *VHL*-mutant RCC both *in vitro* and *in vivo*.

VHL-null/mutant renal tumors are characterized by an angiogenic phenotype due to constitutive HIF2α upregulation as a consequence of loss-of-*VHL* function (25). Hence, the investigation of the regulation of tumor angiogenesis is important in the characterization of effective anticancer compounds and further drug development. We studied the effect of 2HF on angiogenic signaling *in vitro* by examining VEGF expression (26). 2HF treatment caused significant reduction in the levels of VEGF expression in *VHL*-mutant RCC when compared with *VHL*-wild-type RCC (Figure 3B). 2HF treatment lead to specific and significant decrease in angiogenesis as determined by change in both the number and size of cellular tubes formed in *in vitro* tube formation assay in *VHL*-mutant RCC (Figure 3C). Following *in vitro* angiogenic assay, we studied the effect of 2HF on the migratory potential of RCC *in vitro*. 2HF treatment also caused significant inhibition of cell migration in wound-healing assay in *VHL*-mutant RCC (Figure 3D).

2HF inhibits cell cycle progression in VHL-mutant RCC

The mechanism of cytotoxicity of 2HF was further assessed by determining apoptosis through cell cycle fluorescence activated cell sorting analysis. The 50 μM of 2HF treatment for 18 h caused G_2/M phase arrest, which was predominant in *VHL*-mutant RCC (∼61% cells accumulated in G_2 phase, $P < 0.01$) (Figure 4A). Please note that the use of even higher concentration of 2HF (50 μM) in Caki-2 RCC was not effective in inhibiting cell cycle when compared with cell cycle results obtained with 25 μM of 2HF in 786-O RCC. We further analyzed the morphology of RCC cells after 2HF treatment. The *VHL*-mutant and *VHL*-wild-type RCC were treated with 50 μM of 2HF for 24 h and the cell morphology was observed by live cell imaging in Zeiss phase contrast microscope. The 2HF-treated *VHL*-mutant RCC cells were less adherent and more rounded compared with the controls and *VHL*-wild-type RCC. The initial morphological observation of control and 2HF-treated *VHL*-mutant RCC cells indicated impaired cell division in 2HF-treated cells. 2HF-treated *VHL*-mutant RCC cells had more cells that were unable to complete cytokinesis compared with the control cells (Figure 4B). These results confirmed G_2/M phase arrest and potential inhibition of the completion of cytokinesis in 2HF-treated *VHL*-mutant RCC. The 2HF treatment reduced the levels of cyclin B1 and CDK4 in *VHL* mutant but not in *VHL*-wild-type RCC (Figure 4C). Some of the natural anticancer compounds like silibinin are known to cause G_2/M phase arrest by inhibiting cyclin B1 (27). CDK4, commonly associated with G_1 transition, has been also investigated for its role in G_2/M transition and it has been shown that overexpression of dominant-negative CDK4 leads to arrest of G_2 phase progression (28). Some of the anticancer compounds like apigenin and thiomersal also cause inhibition of CDK4 along with cyclin B1 while causing G_2/M phase arrest (29,30). Collectively, our *in vitro* results strongly validated the specific antiproliferative, anti-angiogenic and antimetastatic effects of 2HF in *VHL*-mutant RCC which lead to further investigation of 2HF *in vivo* mice xenografts.

2HF induces potent tumor regression in vivo mice xenografts

VHL-mutant 786-O RCC cells bearing animals with established subcutaneously implanted tumors (∼20 mm^2) were treated with 0.0025, 0.005 and 0.01% (wt/wt) (equivalent to25, 50 and 100 mg/kg body wt,

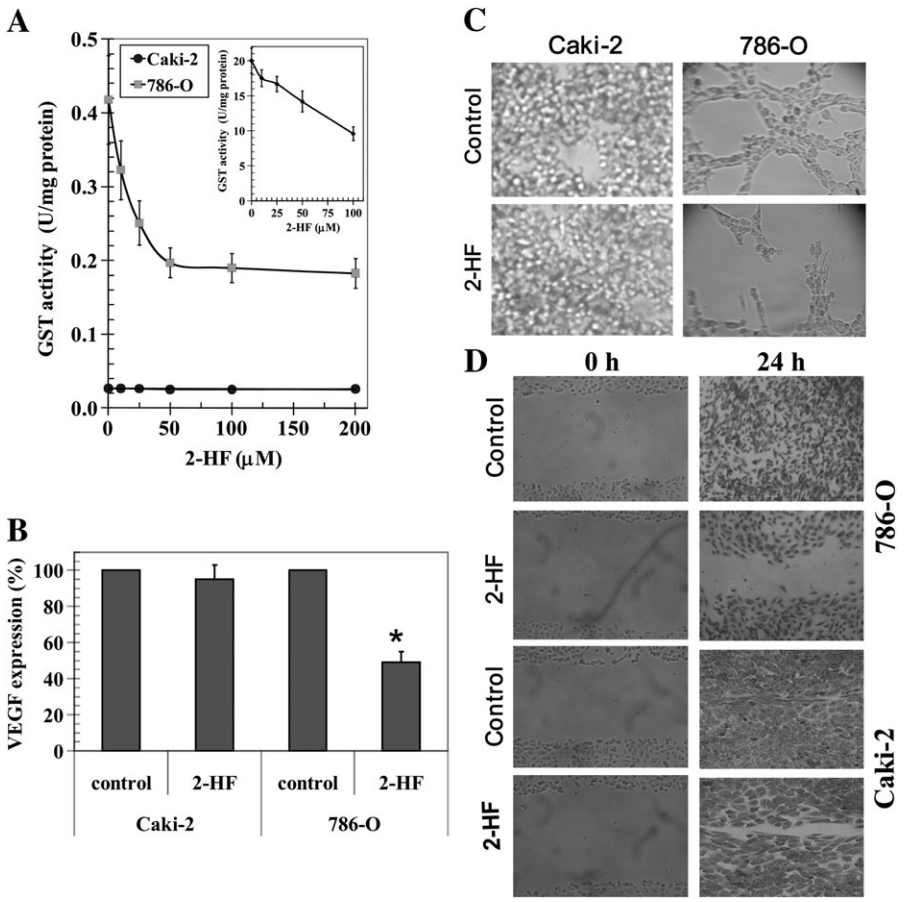

Fig. 3. 2HF inhibits GSTπ activity and angiogenesis. GST activity towards GSH and 1-chloro 2,4-dinitro benzene and its inhibition by 2HF was performed in 28 000*g* crude supernatant prepared from Caki-2 and 786-O cells. Recombinant purified GSTπ was used as a control (panel A and inset). The inhibitory effect of 2HF on GST was studied at a fixed concentration of GSH and GSH and 1-chloro 2,4-dinitro benzene (1 mM each) and varying concentrations of inhibitor. The enzymes were preincubated with the inhibitor for 5 min at 37°C prior to the addition of the substrates (panel A). VEGF expression in control and 2HF-treated cells by enzyme-linked immunosorbent assay kit (R&D System) (panel B). Effect of 2HF (50 μM) on tube formation of Caki-2 and 786-O cells on matrigel was assessed (panel C) and wound-healing assay shows that the 2HF inhibits 786-O cell migration as detailed in Materials and Methods (panel D).

respectively) of 2HF in corn oil by oral gavage on alternate days. In the present studies, doses of 2HF were well tolerated by the mice and did not result in any weight loss compared with age-matched controls (Figure 5A). Photographs of animals were taken at day 1, 10, 20, 40 and 60 after subcutaneous injection. Tumors grew more slowly in *VHL*-mutant RCC mice xenografts administered with 2HF than in respective untreated control mice. At day 60, tumor cross-sectional area and tumor weight of mice bearing *VHL*-mutant RCC was significantly lower in 0.01% (wt/wt) dose-treated group as compared with the vehicle only (corn oil) treated group (19.8 ± 3 versus 122 ± 7 mm^2 and 0.07 ± 0.01 g versus 2.14 ± 0.24 g, respectively; $P < 0.001$). More importantly, *in vivo* studies showed that administration of 2HF at 0.01% (wt/wt), to nude mice-bearing *VHL*-mutant RCC completely arrested tumor progression, whereas uncontrolled growth was observed in the animals treated with vehicle only (Figure 5B and C). The 2HF-treated animals with *VHL*-mutant RCC were still alive at 139 days. In comparison, all animals treated with vehicle only were censored by day 71 ± 3. These results indicated that dietary 2HF administration inhibits *VHL*-mutant RCC growth and prolongs survival without causing side effects. To rule out the possibility that the observed *in vivo* effects of 2HF were specific to *VHL*-mutant RCC, we also evaluated the antineoplastic effects of 2HF on the *VHL*-wild-type (Caki-2) RCC. We observed tumor growth arrest due to 2HF treatment in *VHL*-wild-type RCC but to a lesser extent compared with *VHL*-mutant RCC (at day 60, tumor cross-sectional area and tumor weight, 2HF treated versus control; 98 ± 12 versus 115 ± 7 mm^2 and 1.84 ± 0.12 g versus 2.25 ± 0.18 g, respectively; non-significance) (Figure 5). Also, even 100 mg/kg body wt of 2HF caused only ∼18% reduction in the tumor growth of *VHL*-wild-type Caki-2 RCC, whereas only 25 mg/kg body wt of 2HF caused 41% tumor regression in *VHL*-mutant 786-O RCC ($P < 0.001$).

In our *in vitro* studies, 2HF effectively inhibited the angiogenic process and clonogenic potential besides causing apoptosis in *VHL*-mutant RCC. In order to assess the degree of impact of 2HF *in vivo* on these processes of specific importance in *VHL*-mutant RCC progression and metastasis, we performed histopathological examination of the resected tumor xenografts.

2HF inhibits the expression of proliferative and angiogenic markers while promoting normal epithelial differentiation in VHL-mutant RCC

The histopathological examination of paraffin-embedded tumor xenograft sections as observed by initial hematoxylin and eosin staining revealed that 2HF treatment reduces the number of tumor blood vessels and restores the normal morphology specifically in *VHL*-mutant RCC when compared with controls (Figure 6). Following this observation, we probed the tumor sections for specific markers of proliferation, angiogenesis and differentiation. 2HF treatment decreased the levels of proliferation marker, Ki 67 and angiogenesis marker, CD31, in *VHL*-mutant RCC, which further supported the observed *in vitro* antiproliferative and anti-angiogenic effects of 2HF. Another important finding was that the 2HF treatment predominantly increased the expression of E-cadherin in *VHL*-mutant RCC

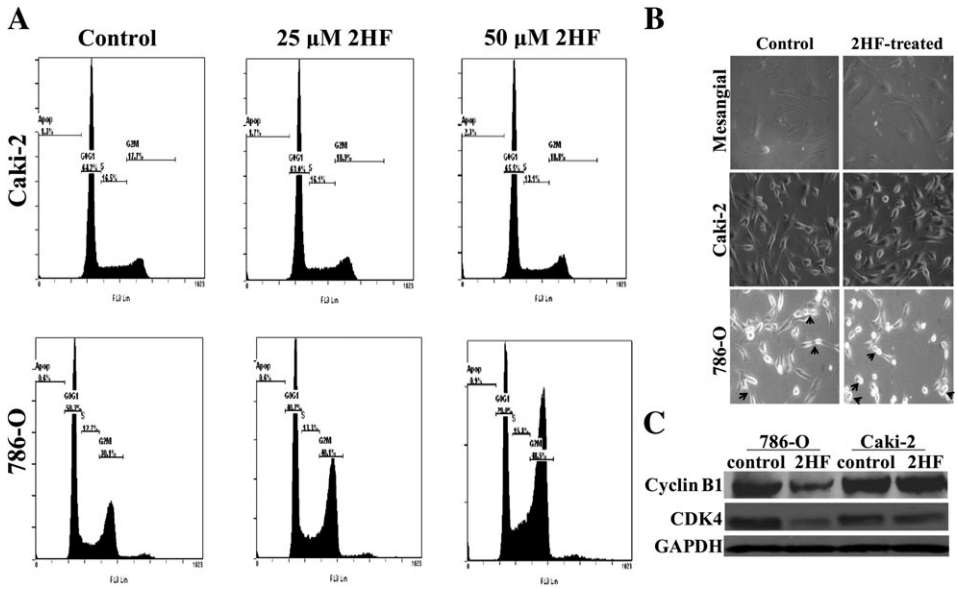

Fig. 4. Effect of 2HF on cell cycle progression in RCC. Inhibitory effect of 2HF on cell cycle distribution was determined by fluorescence activated cell sorting analysis. Experimental details are given in the Methods section. The stained cells were analyzed using the Beckman Coulter Cytomics FC500, Flow Cytometry Analyzer. The experiment was repeated three times and similar results were obtained (panel A). The cell morphology was observed and imaged at ×40 magnification in phase contrast microscope (Axio observer A1; Carl Zeiss microimaging, Thornwood, NY). Arrows in the panel point towards cells arrested in or completing cytokinesis (panel B). *VHL*-wild-type (Caki-2) and *VHL*-mutant (786-O) control and 50 µM 2HF-treated cells were processed for western blot analysis for cyclin B1 and CDK4 expression by using specific antibodies. Membranes were stripped and reprobed for GAPDH as a loading control (panel C).

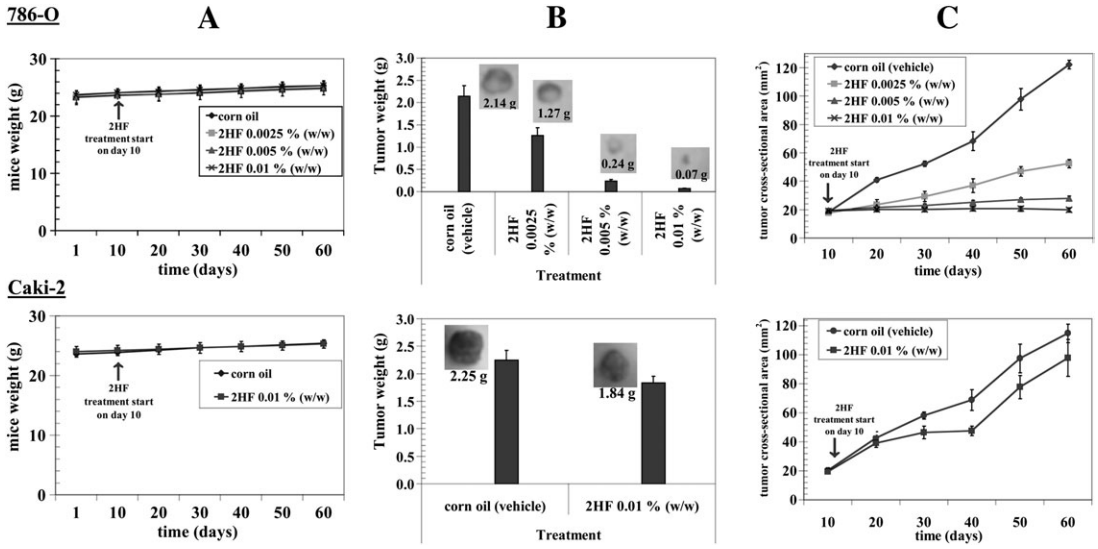

Fig. 5. Effect of oral administration of 2HF on tumor regression of RCC in nude mice: For 786-O RCC, mice were divided into four groups treated with corn oil (i.e. vehicle) and 2HF 0.0025, 0.005 and 0.01% (wt/wt) (equivalent to 25, 50 and 100 mg/kg body wt, respectively). For Caki-2 RCC, mice were divided into two groups treated with corn oil, and 2HF 0.01% (wt/wt) (equivalent to 100 mg/kg body wt). Experimental details are given in the Methods section. Animals were examined daily for signs of tumor growth and body weights were recorded (panels A). Photographs of animals were taken at day 1, day 10, day 20, day 40 and day 60 after subcutaneous injection are shown for all groups (data not shown). Weights and photographs of tumors were also taken at day 60 (panels B). Tumors were measured in two dimensions using calipers (panels C).

xenografts. E-cadherin is considered a suppressor of invasion and growth of many epithelial cancers because of its role in the inhibition of epithelial–mesenchymal transition (EMT) and promoting normal epithelial phenotype (31–34). E-cadherin is frequently downregulated during cancer progression and correlates with poor prognosis (35). Loss of E-cadherin is associated with incidence and progression of many epithelial tumors (35–37). In this regard, overexpression of E-cadherin consequent to 2HF treatment represents a highly significant and novel mechanism of action of 2HF in *VHL*-mutant RCC (Figure 6).

Discussion

RCC is one of the frequently incident cancers in USA with an increasing current trend of incidence. Intake of citrus fruits has been shown to reduce RCC risk in clinical trials (9). In this regard, we investigated the anticancer effects and the respective mechanisms of action of 2HF, a natural compound found in citrus fruits and oranges, in RCC. Our studies demonstrate that 2HF exhibits potent antiproliferative and pro-apoptotic effects to a significantly greater extent in *VHL*-mutant RCC when compared with *VHL*-wild-type RCC. The

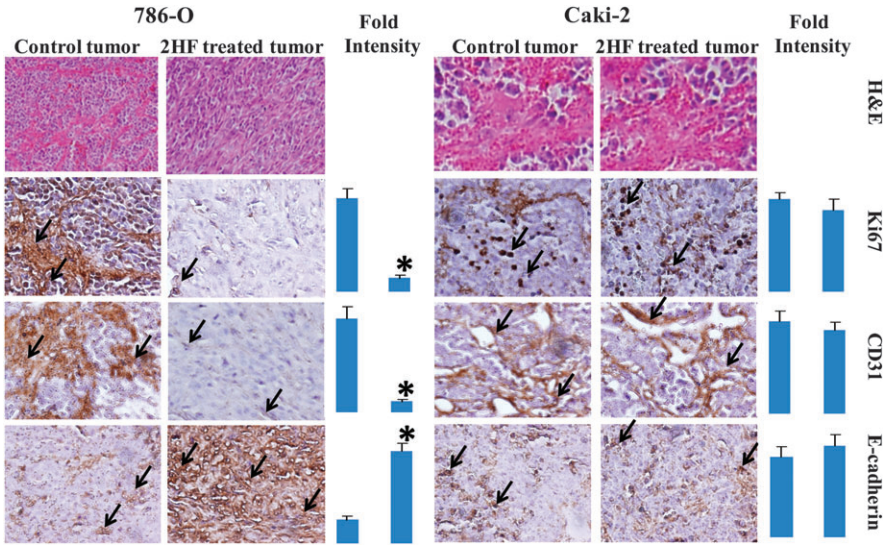

Fig. 6. Histopathologic analyses of the markers of proliferation, angiogenesis and differentiation in tumor sections after 2HF treatment. Control and 2HF-treated RCC-bearing nude mice tumor sections were used for histopathologic analyses. Presented are hematoxylin and eosin stained sections, immuno-histochemistry analyses for Ki-67 expression (marker of cellular proliferation), CD31 (angiogenesis marker) and E-cadherin (tumor suppressor) from tumors in mice of control and 2HF-treated groups. Statistical significance of difference was determined by two-tailed Student's *t*-test. $P < 0.001$, 786-O 2HF-treated compared with control. However, these differences were not significant in Caki-2. Immunoreactivity is evident as a dark brown stain, whereas non-reactive areas display only the background color. Sections were counterstained with hematoxylin (blue). Photomicrographs at ×40 magnification were acquired using Olympus Provis AX70 microscope. Percent staining was determined by measuring positive immunoreactivity per unit area. Arrows represent the area for positive staining for an antigen. The intensity of antigen staining was quantified by digital image analysis. Bars represent mean ± standard error ($n = 5$); $^{*}P < 0.001$ compared with control.

antiproliferative effects of 2HF were mediated by the inhibition of EGFR, PI3K and pAkt signaling in *VHL*-mutant RCC. The growth inhibitory effects of 2HF also included the inhibition of cell cycle progression, which was mediated by reduction in the levels of cyclin B1 and CDK4 in *VHL*-mutant RCC.

2HF was shown in our studies, for the first time, to be a novel GSTπ inhibitor. 2HF also effectively inhibited both recombinant GSTπ and >50% of total GST activity in *VHL*-mutant RCC at concentrations toxic to tumors but well tolerated by normal cells. Posttranslational S-glutathionylation of proteins which is an emerging topic of investigation in apoptosis and enhanced oxidative signaling due to constitutively active HIF2α in *VHL*-null background signify the role of GSTπ function in regulating differential cytotoxicity of 2HF in RCC. Enhanced expression of GSTπ can lead to increased detoxification of products of lipid peroxidation and administered chemotherapy drugs by conjugation with glutathione (GSH) to form glutathione adducts (GS-E) which are eventually transported out of the cells by an active, ATP dependent process mediated by the membrane transporter, RLIP76 or Ral-binding protein 1 (RalBP1) (14–16). GSTπ also catalyzes the S-glutathionylation of active site nucleophilic cysteines in many phosphatases conferring additional negative charge to the active site (24). S-glutathionylation induced redistribution of charge at active site of proteins has been known to influence both substrate accessibility and catalytic efficiency of target proteins with pronounced effects on the tumor-signaling pathways (38). In this regard, further knockin and knockout follow-up studies of GSTπ, *VHL* and HIF2α could characterize the impact of differential regulation of oxidative stress pathways in regulating the anticancer effects of 2HF.

One of the significant observation was that 2HF caused effective inhibition of VEGF expression in *VHL*-mutant RCC sparing normal mesangial cells. Angiogenesis is essential for the growth of rapidly proliferating tumors whose centers are usually hypoxic and specifically in renal tumors with *VHL* mutations, which have high HIF2α levels. HIF2α initiates a compensatory angiogenic response to match the rapid rate of tumor growth by stimulating VEGF expression (39). Normally, *VHL* binds to HIF2α and targets it for degradation. Loss or inactivation of *VHL* leads to loss of substrate recognition required for binding to HIF2α which effectively leads to enhanced levels and activity of HIF2α and consequent tumor angiogenesis (40,41). In this regard, 2HF represents a safe and novel anti-angiogenic natural compound without normal tissue cytotoxicity with specific significance in the management of highly vascular *VHL*-mutant RCC.

Our *in vivo* studies further provided corroborative evidence to the anticancer effects and mechanisms of action of 2HF of particular relevance to *VHL*-mutant RCC. It is possible that potential pharmacokinetic differences in drug uptake and metabolism between cell types which in turn influence the duration of drug action at intracellular targets could be contributing to some of the terminal events due to 2HF treatment between the *VHL*-wild-type and *VHL*-mutant genotypes of RCC which need further absorption, distribution, metabolism and excretion (ADME) studies. However, from a clinical point of view, the ability of 2HF to effectively target *VHL*-mutant RCC, which contributes to most common form of RCCs is of potential significance in the chemoprevention of RCC. Our mice xenograft studies also confirmed that the orally administered 2HF is effective *in vivo* to exert its anticancer effects in *VHL*-mutant RCC as observed similarly in the *in vitro* studies. The dose of 2HF required to cause effective tumor regression (∼90% reduction in tumor growth, Figure 5) in *VHL*-mutant RCC was 0.01% (wt/wt), which is well in comparable range to other flavonoids being tested in clinical trials (27). Also, 2HF caused inhibition of Akt signaling and increased poly ADP-ribose polymerase-cleavage in mice xenografts of *VHL*-mutant RCC, which revealed that the orally administered 2HF can effectively induce an *in vivo* antimitogenic and pro-apoptotic response (data not shown). 2HF also decreased the expression of proliferative marker, Ki 67 and angiogenic marker, CD31, in the *VHL*-mutant RCC. One of the significant findings was that 2HF treatment increased the levels of E-cadherin specifically in *VHL*-mutant tumors *in vivo*. Loss of E-cadherin is associated with incidence and progression of many epithelial tumors and restoration of E-cadherin reverts them to normal epithelial phenotype (42). Given the renal tubular epithelial origin of RCC, the increased expression of E-cadherin after 2HF treatment assumes mechanistic significance in the chemoprevention of *VHL*-mutant RCC.

VHL syndrome is an autosomal dominant condition caused by mutation or deletion of the *VHL* gene and characterized by highly vascular neoplasms including RCC, café-au-lait spots, angiomatosis, hemangioblastomas and pheochromocytomas. *VHL* protein is an

ubiquitin E3 ligase that targets HIF to proteasomal degradation and thus prevents constitutive activation of hypoxic and angiogenic signaling (43). Our findings providing strong evidence for the pro-apoptotic, anti-angiogenic and pro-differentiation effects of 2HF in *VHL*-mutant RCC could also have additional potential implications towards other *VHL*-related tumor syndromes in general. Taken together, in the light of pathogenetic mechanisms of loss-of-*VHL* driven renal carcinogenesis, the anticancer properties of 2HF like inhibition of survival, proliferation and tumor vascularization without causing any overt toxicity towards normal tissues provide sound scientific rationale for the role of 2HF in the chemoprevention of *VHL*-mutant RCC.

Funding

This work was supported by the National Institutes of Health grant (CA 77495 to S.A. & S.S.S.) and ISIORR018999-01A1; the Welch Foundation endowment (BK-0031 to L.P.); the Cancer Research Foundation of North Texas; Institute for Cancer Research & the Joe & Jessie Crump Fund for Medical Education to S.S.S.

Acknowledgements

The authors thank Dr Xiangle Sun, core facility at the University of North Texas Health Science Center, Fort Worth, TX, for helping with flow cytometry and laser capture microdissection (supported by NIH Grant ISIORR018999-01A1). We also thank Dr Sumihiro Suzuki, Department of Biostatistics, School of Public Health, University of North Texas Health Science Center, Fort Worth, TX, for his assistance in the statistical analyses of the data.

Conflict of Interest Statement: None declared.

References

1. Linehan,W.M. *et al*. (2004) Genetic basis of cancer of the kidney: disease-specific approaches to therapy. *Clin. Cancer Res.*, **10**, 6282S–6289S.
2. Atkins,M.B. *et al*. (2007) Innovations and challenges in renal cell carcinoma: summary statement from the Second Cambridge Conference. *Clin. Cancer Res.*, **13**, 667s–670s.
3. Kuroda,N. *et al*. (2003) Review of renal oncocytoma with focus on clinical and pathobiological aspects. *Histol. Histopathol.*, **18**, 935–942.
4. Hunt,J.D. *et al*. (2005) Renal cell carcinoma in relation to cigarette smoking: meta-analysis of 24 studies. *Int. J. Cancer.*, **114**, 101–108.
5. Van Dijk,B.A. *et al*. (2006) Cigarette smoking, von Hippel-Lindau gene mutations and sporadic renal cell carcinoma. *Br. J. Cancer.*, **95**, 374–377.
6. Choquenet,B. *et al*. (2009) Flavonoids and polyphenols, molecular families with sunscreen potential: determining effectiveness with an in vitro method. *Nat. Prod. Commun.*, **4**, 227–230.
7. Woodman,O.L. *et al*. (2004) Vascular and anti-oxidant actions of flavonols and flavones. *Clin. Exp. Pharmacol. Physiol.*, **31**, 786–790.
8. Benavente-Garcia,O. *et al*. (2008) Update on uses and properties of citrus flavonoids: new findings in anticancer, cardiovascular, and anti-inflammatory activity. *J. Agric. Food Chem.*, **56**, 6185–6205.
9. Wolk,A. *et al*. (1996) International renal cell cancer study. VII. Role of diet. *Int. J. Cancer.*, **65**, 67–73.
10. Hsiao,Y.C. *et al*. (2007) Flavanone and 2'-OH flavanone inhibit metastasis of lung cancer cells via down-regulation of proteinases activities and MAPK pathway. *Chem. Biol. Interact.*, **167**, 193–206.
11. Singhal,S.S. *et al*. (1992) Glutathione S-transferases of human lung: characterization and evaluation of the protective role of the alpha-class isozymes against lipid peroxidation. *Arch. Biochem. Biophys.*, **299**, 232–241.
12. Prokai,L. *et al*. (2009) Rapid label-free identification of estrogen-induced differential protein expression *in vivo* from mouse brain and uterine tissue. *J. Proteome Res.*, **8**, 3862–3871.
13. Singhal,S.S. *et al*. (2010) Rlip76 transports sunitinib and sorafenib and mediates drug resistance in kidney cancer. *Int. J. Cancer.*, **126**, 1327–1338.
14. Singhal,S.S. *et al*. (2009) RLIP76: a target for kidney cancer therapy. *Cancer Res.*, **69**, 4244–4251.
15. Singhal,S.S. *et al*. (2008) Hsf-1 and POB1 induce drug sensitivity and apoptosis by inhibiting Ralbp1. *J. Biol. Chem.*, **283**, 19714–19729.
16. Singhal,J. *et al*. (2008) RLIP76 in defense of radiation poisoning. *Int. J. Radiat. Oncol. Biol. Phys.*, **72**, 553–561.
17. Rosenberg Zand,R.S. *et al*. (2002) Flavonoids can block PSA production by breast and prostate cancer cell lines. *Clin. Chim. Acta.*, **317**, 17–26.
18. Lee,S.J. *et al*. (2008) Von Hippel-Lindau tumor suppressor gene loss in renal cell carcinoma promotes oncogenic epidermal growth factor receptor signaling via Akt-1 and MEK-1. *Eur. Urol.*, **54**, 845–853.
19. Merseburger,A.S. *et al*. (2008) Activation of PI3K is associated with reduced survival in renal cell carcinoma. *Urol. Int.*, **80**, 372–377.
20. Skarydova,L. *et al*. (2009) AKR1C3 as a potential target for the inhibitory effect of dietary flavonoids. *Chem. Biol. Interact.*, **178**, 138–144.
21. Ritchie,K.J. *et al*. (2007) Glutathione transferase pi plays a critical role in the development of lung carcinogenesis following exposure to tobacco-related carcinogens and urethane. *Cancer Res.*, **67**, 9248–9257.
22. Kollermann,J. *et al*. (2006) Impact of hormonal therapy on the detection of promoter hypermethylation of the detoxifying glutathione-S-transferase P1 gene (GSTP1) in prostate cancer. *BMC Urol.*, **6**, 15.
23. Awasthi,Y.C. *et al*. (2008) Self-regulatory role of 4-hydroxynonenal in signaling for stress-induced programmed cell death. *Free Radic. Biol. Med.*, **45**, 111–118.
24. Barrett,W.C. *et al*. (1999) Regulation of PTP1B via glutathionylation of the active site cysteine 215. *Biochemistry.*, **38**, 6699–6705.
25. Ohh,M. *et al*. (2000) Ubiquitination of hypoxia-inducible factor requires direct binding to the beta-domain of the von Hippel-Lindau protein. *Nat. Cell Biol.*, **2**, 423–427.
26. Leung,D.W. *et al*. (1989) Vascular endothelial growth factor is a secreted angiogenic mitogen. *Science/*, **246**, 1306–1309.
27. Tyagi,A.K. *et al*. (2002) Silibinin strongly synergizes human prostate carcinoma DU145 cells to doxorubicin-induced growth Inhibition, G2-M arrest, and apoptosis. *Clin. Cancer Res.*, **8**, 3512–3519.
28. Gabrielli,B.G. *et al*. (1999) A cyclin D-Cdk4 activity required for G2 phase cell cycle progression is inhibited in ultraviolet radiation-induced G2 phase delay. *J. Biol. Chem.*, **274**, 13961–13969.
29. Yin,F. *et al*. (2001) Apigenin inhibits growth and induces G2/M arrest by modulating cyclin-CDK regulators and ERK MAP kinase activation in breast carcinoma cells. *Anticancer Res.*, **21**, 413–420.
30. Woo,K.J. *et al*. (2006) Thimerosal induces apoptosis and G2/M phase arrest in human leukemia cells. *Mol. Carcinog.*, **45**, 657–666.
31. Scholzen,T. *et al*. (2000) The Ki-67 protein: from the known and the unknown. *J. Cell. Physiol.*, **182**, 311–322.
32. Folkman,J. (1971) Tumor angiogenesis: therapeutic implications. *N. Engl. J. Med.*, **285**, 1182–1186.
33. Wheelock,M.J. *et al*. (2003) Cadherins as modulators of cellular phenotype. *Annu. Rev. Cell Dev. Biol.*, **19**, 207–235.
34. Yang,J. *et al*. (2008) Epithelial-mesenchymal transition: at the crossroads of development and tumor metastasis. *Dev. Cell.*, **14**, 818–829.
35. Mohammadizadeh,F. *et al*. (2009) Correlation of E-cadherin expression and routine immunohistochemistry panel in breast invasive ductal carcinoma. *Cancer Biomark.*, **5**, 1–8.
36. Cheng,J.C. *et al*. (2010) Hydrogen peroxide mediates EGF-induced down-regulation of E-cadherin expression via p38 MAPK and snail in human ovarian cancer cells. *Mol. Endocrinol.*, **24**, 1569–1580.
37. Hu,J. *et al*. (2010) Hepatocyte growth factor induces invasion and migration of ovarian cancer cells by decreasing the expression of E-cadherin, beta-catenin, and caveolin-1. *Anat. Rec. (Hoboken)*, **293**, 1134–1139.
38. Xie,Y. *et al*. (2009) S-glutathionylation impairs signal transducer and activator of transcription 3 activation and signaling. *Endocrinology.*, **150**, 1122–1131.
39. Nilsson,M.B. *et al*. (2010) Multiple receptor tyrosine kinases regulate HIF-1alpha and HIF-2alpha in normoxia and hypoxia in neuroblastoma: implications for antiangiogenic mechanisms of multikinase inhibitors. *Oncogene.*, **29**, 2938–2949.
40. Del Rey,M.J. *et al*. (2009) Human inflammatory synovial fibroblasts induce enhanced myeloid cell recruitment and angiogenesis through a hypoxia-inducible transcription factor 1alpha/vascular endothelial growth factor-mediated pathway in immunodeficient mice. *Arthritis Rheum.*, **10**, 2926–2934.
41. Kumar,A. *et al*. (2009) Antiangiogenic and antiproliferative effects of substituted-1,3,4-oxadiazole derivatives is mediated by down regulation of VEGF and inhibition of translocation of HIF-1alpha in Ehrlich ascites tumor cells. *Cancer Chemother. Pharmacol.*, **6**, 1221–1233.
42. Almeida,P.R. *et al*. (2010) E-cadherin immunoexpression patterns in the characterisation of gastric carcinoma histotypes. *J. Clin. Pathol.*, **63**, 635–639.
43. Kaelin,W.G.Jr. (2008) The von Hippel-Lindau tumour suppressor protein: O2 sensing and cancer. *Nat. Rev. Cancer.*, **8**, 865–873.

Received December 1, 2010; revised January 12, 2011; accepted January 22, 2011